

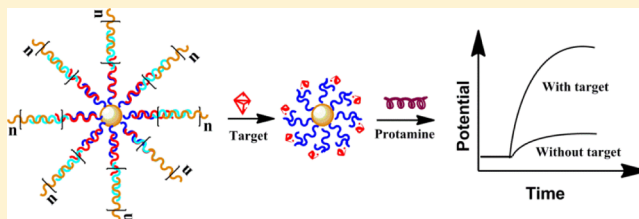
# DNA Nanostructure-Based Magnetic Beads for Potentiometric Aptasensing

Jiawang Ding, Yue Gu, Fei Li, Hongxia Zhang, and Wei Qin\*

Key Laboratory of Coastal Environmental Processes and Ecological Remediation and Shandong Provincial Key Laboratory of Coastal Environmental Processes, Yantai Institute of Coastal Zone Research (YIC), Chinese Academy of Sciences (CAS), Yantai, Shandong 264003, P. R. China

## Supporting Information

**ABSTRACT:** In this work, a simple, general, and sensitive potentiometric platform is presented, which allows potentiometric sensing to be applied to any class of molecule irrespective of the analyte charge. DNA nanostructures are self-assembled on magnetic beads via the incorporation of an aptamer into a hybridization chain reaction. The aptamer–target binding event leads to the disassembly of the DNA nanostructures, which results in a dramatic change in the surface charge of the magnetic beads. Such a surface charge change can be sensitively detected by a polycation-sensitive membrane electrode using protamine as an indicator. With an endocrine disruptor bisphenol A as a model, the proposed potentiometric method shows a wide linear range from 0.1 to 100 nM with a low detection limit of 80 pM ( $3\sigma$ ). The proposed sensing strategy will lay a foundation for the development of potentiometric sensors for highly sensitive and selective detection of various targets.



In the past two decades, modern potentiometry with ion-selective electrodes (ISEs) has gained considerable attention owing to the large improvement in the detection limit and selectivity coefficients.<sup>1</sup> With the introduction of novel sensing concepts, ISEs have evolved to be a promising technique for ion sensing.<sup>2,3</sup> To date, various methods including low detection limit ISEs,<sup>4</sup> polyion sensors,<sup>5</sup> chronopotentiometric detection,<sup>6</sup> controlled reagent release,<sup>7</sup> coulometric analysis,<sup>8</sup> and nanopore sensors have been proposed in the field of ISEs.<sup>9</sup> However, most of the successful applications of ISEs are still limited to detection of a number of ionic species, and low levels of electrolyte backgrounds are usually required for the low detection limit measurements.<sup>10,11</sup> It thus remains a challenge to apply potentiometric sensors to detect a broad range of different molecular targets with high sensitivity, especially in complex media (e.g., clinical or environmental samples).

DNA or RNA aptamers have emerged as an alternative bioreceptor for biosensing in lieu of antibodies. Up to now, aptamers for a variety of analytes ranging from small ions to large proteins or even whole cells are available.<sup>12</sup> Electrochemical aptasensors using aptamers as biorecognition elements have been extensively investigated.<sup>13</sup> Most of these sensors are however based on amperometry and impedimetry, and potentiometric aptasensors are still rather rare. An aptamer-based potentiometric sandwich assay format based on nanoparticle labels (i.e., semiconductor nanocrystals) was developed by using miniaturized ion-selective electrodes that exhibit attractive detection limits in confined sample volumes.<sup>14</sup> This approach is promising for protein assays but may not be suitable for measurements of small molecules since their secondary aptamers are often unavailable. Potentiometric

aptasensing of living bacteria was proposed based on the target-induced surface charge change of shielded carbon nanotubes or graphene.<sup>15</sup> This method is simple and rapid but may suffer from problems of the strong interference from electrolyte background and small potential signals. Recently, a label-free and substrate-free potentiometric aptasensing strategy was developed, which allows the measurements to be performed in a homogeneous solution.<sup>16,17</sup> In this method, signal transduction is based on the binding-induced conformational change of the aptamer, which is however a condition that cannot always be easily achieved.

Herein, we present a novel potentiometric sensing platform that couples to a signal amplification strategy based on DNA assembly. DNA self-assembly processes such as hybridization chain reactions (HCRs) provide simple and effective biotechnologies for in situ formation of long-range DNA nanostructures.<sup>18</sup> Indeed, HCRs have been successfully employed in aptasensors for signal amplification using reporters such as fluorophores, redox tags, intercalators, DNAzymes, nanoparticles, and ions.<sup>19–23</sup> In this work, a general and highly sensitive potentiometric aptasensing strategy is proposed based on incorporation of a DNA aptamer into the HCR event. Unlike previous HCR-sensing modes which always require signal reporters, the proposed method allows DNA to be potentiometrically detected as a polyanion by a polycation-sensitive membrane electrode using protamine as an indicator.

Received: April 26, 2015

Accepted: June 5, 2015

Published: June 5, 2015

Complex DNA nanostructures that contain multiple or single target-binding site are designed. Magnetic beads (MBs), which can be adopted as a multifunctional assay platform,<sup>24</sup> are conjugated to the aptamer to eliminate the interfering effect from the sample matrix. The analyte binding induced disassembly of the DNA nanostructures results in a dramatic change in the surface charge of magnetic beads, which can be measured by the polycation membrane electrode. It will be shown that the aptasensing strategy described herein provides an optimal combination of generality and sensitivity that is currently unmatched by other potentiometric aptasensors and can be used for potentiometric detection of a wide range of targets.

## EXPERIMENTAL SECTION

### Membrane Preparation and EMF Measurements.

Polycation-sensitive electrode membranes containing 1.0 wt % DNNS, 1.0 wt % ETH 500, 49.0 wt % *o*-NPOE, and 49.0 wt % PVC were prepared as described before.<sup>17</sup> All the measurements were carried out at  $25 \pm 2$  °C using a Model PXSJ-216 digital ion analyzer (Shanghai Leici Instruments Factory, China). Measurements of electromotive force (EMF) were performed in the galvanic cell: Ag/AgCl/3 M KCl/0.1 M LiOAc/sample solution/ISE membrane/inner filling solution/AgCl/Ag. 50 mM pH 7.4 Tris–HCl buffer solution containing 0.12 M NaCl was used as the inner filling solution. The potential responses were measured by a polycation-sensitive membrane electrode with a rotating electrode configuration (3000 rpm) as described before (see the Supporting Information).<sup>11</sup> Before measurements, the electrodes were conditioned in 0.01 M NaCl for 5 min to obtain a stable baseline.

**DNA Self-Assemblies on Magnetic Beads.** The bisphenol A (BPA) aptamer or linker DNA fragments were immobilized on magnetic beads according to the procedures of the xMag PDITC Oligo Immobilization Starter Kit (Xi'an GoldMag Nanobiotech Company, Ltd.). The details for DNA self-assemblies on magnetic beads were described in the Supporting Information.

**BPA Detection.** Thirty  $\mu\text{L}$  BPA solutions at different concentrations were incubated with 30  $\mu\text{L}$  of DNA self-assembled magnetic beads in the binding buffer for 1 h. After magnetic separation, the MBs were washed twice with the buffer and dispersed into 30  $\mu\text{L}$  of 0.2 mg mL<sup>-1</sup> protamine in 0.01 M sodium chloride. After incubation for 5 min and magnetic separation, the residual protamine solution was added to 2.97 mL of 0.01 M sodium chloride for potentiometric measurements. The potential differences between the baseline and the potentials measured at 80 s were used for quantification of BPA.

## RESULTS AND DISCUSSION

The sensing principle is illustrated in Figure 1. For protocol A, an aptamer can hybridize with a capture DNA linker immobilized on magnetic beads to form a double-stranded DNA (see Table S1, Supporting Information, for the sequences of synthesized oligonucleotides). When the target is present in the sample solution, the aptamer–target binding interaction could induce the aptamer release from the magnetic beads and thus reduce the DNA amount (i.e., negative charges) on the bead surface. In this protocol, a single target molecule induces a single DNA fragment release, which restricts its sensitivity. The

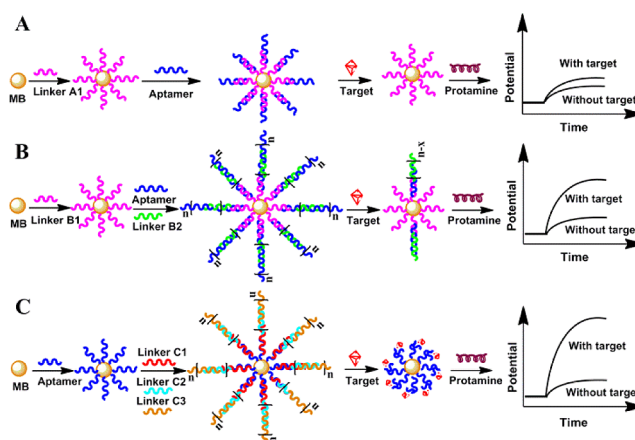


**Figure 1.** Schematic illustration of the DNA nanostructure-based magnetic beads for potentiometric aptasensing. For protocol A, a DNA linker is bound to the surface of magnetic beads to hybridize with the short aptamer. For protocol B, linker B1 is bound to the surface of magnetic beads to initiate the HCR in the presence of the short aptamer and linker B2. For protocol C, the long aptamer is tethered to the surface of magnetic beads. Linker C1 is used to initiate the HCR in the presence of two auxiliary probes (linkers C2 and C3).

sensing performance can be largely improved by integrating more complex DNA nanostructures via HCRs for signal amplification, as shown in protocols B and C. For protocol B, numerous aptamer fragments are involved in the construction of the supersandwich form in the presence of the aptamer and its linkers. A DNA sequence (linker B1) is bound to the surface of magnetic beads to initiate the HCR. The capture DNA (linker B2) can hybridize to either lateral portion of the aptamer thus creating the long concatamers containing multiple aptamer fragments. The target molecules can bind to the aptamer sequences in the concatamers randomly, which leads to a partial disassembly of the nanostructures. For protocol C, the aptamer is tethered to the surface of magnetic beads. The two auxiliary DNA fragments (linkers C2 and C3) can initiate a cascade of the hybridization event and lead to the formation of long-range DNA nanostructures. The aptamer and long-range DNA nanostructures are connected with linker C1. In the presence of the analyte, the aptamer fragments bind specifically to the target molecules. The induced strand displacement can cause a complete disassembly of the DNA nanostructures. The change in the charge or DNA concentration on the magnetic bead surface can be monitored by a polycation-sensitive membrane electrode using protamine as an indicator. Bisphenol A, an endocrine disruptor with widespread exposure and multiple effects, was selected as a model target. An aptamer sequence toward BPA with a dissociation constant of  $8.3 \times 10^{-9}$  M, which is even lower than that of an antibody, was used in the experiment.<sup>25</sup>

The aptamer or linker DNA fragments were immobilized on magnetic beads according to the procedures of the xMag PDITC Oligo Immobilization Starter Kit. Uniformly distributed magnetic beads with an average particle size of ca. 450 nm were used in this work (see Figure S1 in the Supporting Information). The supersandwich structures were constructed according to the reported procedures with some modifications (see the Supporting Information for experimental details).<sup>20</sup>

The DNA nanostructures were verified by UV–vis spectroscopy and gel electrophoresis. As shown in Figure 2A, the self-assembly of DNA on the magnetic beads leads to the decrease

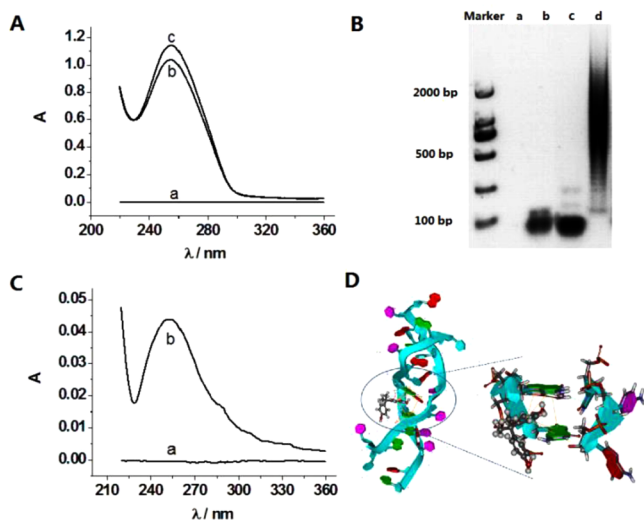


**Figure 2.** (A) UV-vis spectroscopy of (a) the blank (hybridization buffer), (b) the HCR solution after incubation with 400  $\mu\text{L}$  of the aptamer-linker C1 modified magnetic beads for 2 h, and (c) the HCR solution alone. The HCR solution was formed by incubation of 1  $\mu\text{M}$  of linker C2 with that of linker C3 in the hybridization buffer for 1.5 h. (B) Agarose gel electrophoresis: 2000 mer DNA marker; (a) the blank, (b) linker C2, (c) linker C3, and (d) linkers C2 + C3 (i.e., the HCR solution). (C) Absorbance spectra of (a) the blank (the binding buffer) and (b) the DNA fragments released from 200  $\mu\text{L}$  of magnetic beads by  $10^{-6}$  M BPA. (D) DNA structure after binding to the BPA molecule obtained by the molecular docking simulation. The blue ribbons stand for the structure of DNA, the green dotted lines for the H-bonds, and the solid yellow lines for the  $\pi$ - $\pi$  interactions.

in the concentration of DNA in the sample solution, since the DNA fragments are consumed for the formation of the supersandwich structures on the magnetic beads (as illustrated for protocol C). Such supersandwich structures were confirmed by gel electrophoresis. As shown in Figure 2B, a ladder of mixed sandwich structures was formed in the presence of linkers C2 and C3 with a maximum length of more than 2000 base pairs (bp).

The displacement of DNA linkers is the key to achieve highly sensitive and selective detection in this research. The affinity constant for BPA binding to the aptamer sequence is  $1.2 \times 10^8 \text{ M}^{-1}$ ,<sup>25</sup> which is ca. 1 order of magnitude larger than that for the DNA/DNA binding.<sup>26</sup> In this case, the BPA molecules bind to the aptamer fragments more strongly, which leads to the displacement of the DNA linkers and disassembly of the supersandwich structures. As proved by the UV-vis spectroscopy (Figure 2C), the DNA nanostructures are largely diminished (i.e., released from the magnetic beads into the solution) after treatment with BPA. Molecular simulation was also performed to study the interactions of the small molecules of BPA with the biomacromolecules of DNA (see the Supporting Information).<sup>27</sup> The molecular docking analysis reveals that the DNA double helix structure is indeed uncoiled in the presence of BPA (Figures 2D and S2).

Protamine, a group of arginine-rich polycationic proteins, can electrostatically interact with the negatively charged DNA sequences and be used as an indicator for potentiometric aptasensing using a polycation-sensitive membrane electrode.<sup>17</sup> In this work, the supersandwich DNA structures which determine the surface charge or concentration of DNA on the magnetic beads can electrostatically bind to the protamine domain. The presence of the analyte of interest induces the

displacement of the DNA strands in the DNA-aptamer complexes, thus releasing the preformed supersandwich structures from the magnetic bead surface into the solution. The change in the amount of DNA on the magnetic beads can be sensed potentiometrically by using protamine as the indicator. Potentiometric detection was carried out using a rotating electrode configuration to greatly improve the sensitivity of the polycation sensor.

The polycation-selective membrane electrode shows a nonequilibrium steady-state potential response to protamine via the formation of cooperative ion pairs between protamine and the lipophilic exchanger (i.e., DNNS) in the membrane.<sup>28</sup> As shown in Figure 3A, higher potential responses to protamine

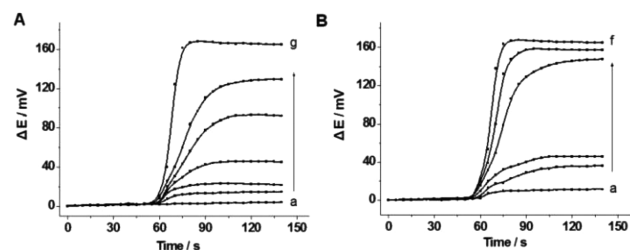


**Figure 3.** Potentiometric responses of the polycation-sensitive membrane electrode in 3.0 mL of 0.01 M NaCl (A) with (a) 0, (b) 0.33, (c) 0.67, (d) 1.0, (e) 1.3, (f) 1.6, and (g) 2.0  $\mu\text{g mL}^{-1}$  protamine and (B) with 2.0  $\mu\text{g mL}^{-1}$  protamine in the presence of (a) 40, (b) 30, (c) 20, (d) 10, (e) 5, and (f) 0  $\mu\text{L}$  of the functionalized magnetic beads prepared according to protocol C.

in 0.01 M NaCl can be obtained in the concentration range of 0.33–2.0  $\mu\text{g mL}^{-1}$ . At concentrations higher than 2.0  $\mu\text{g mL}^{-1}$ , a true equilibrium can be reached at the sample-membrane phase boundary, which renders the polymeric membrane insensitive to protamine. In this work, 2.0  $\mu\text{g mL}^{-1}$  protamine with high sensitivity was used to indicate the aptamer-target binding events.

The positively charged guanidinium groups of protamine binds electrostatically with the negatively charged phosphate groups of DNA fragments.<sup>29</sup> Therefore, the potential response of the membrane electrode would decrease in the presence of DNA nanostructures due to the decrease in the concentration of free protamine in solution. Figure 3B shows that 30  $\mu\text{L}$  of the magnetic beads conjugated with DNA supersandwich structures can dramatically reduce the potential responses, and no obvious potential signal is observed when 40  $\mu\text{L}$  of the functionalized magnetic beads is used.

Since the target-binding induced disassembly of DNA complex structures reduces the anionic sites on the magnetic beads for protamine, more protamine would be available in the test solution, which can be sensed potentiometrically by using the polycation-sensitive electrode. The efficiencies of converting the binding events to the output potentials via different sensing protocols were investigated. As shown in Figure 4A, protocol A shows a much lower sensitivity due to the relatively few released DNA molecules in the presence of the target. In contrast, complex DNA nanostructures that contain single or multiple target-binding sites can provide an amplification mechanism. Compared with protocol B using the DNA nanostructures with multiple target-binding sites, protocol C displays a significant increase in potential response. The improvement can be attributed to the complete release of the complex DNA nanostructures induced by the aptamer binding

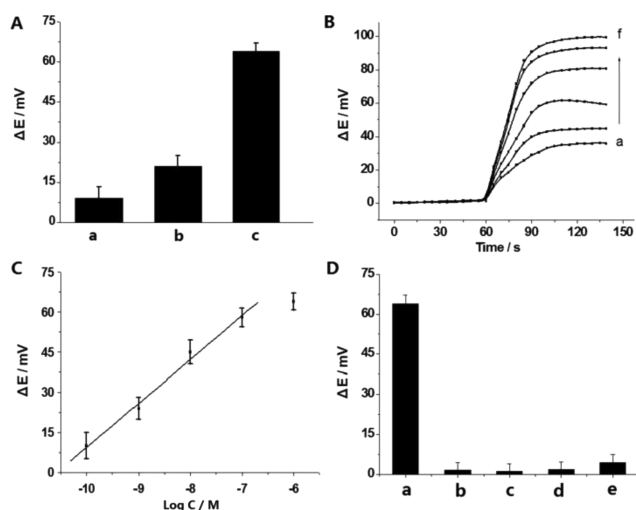


**Figure 4.** (A) Potentiometric responses of the electrode to  $10^{-6}$  M BPA for protocols A (a), B (b), and C (c). (B) Potentiometric responses of the polycation-sensitive membrane electrode in 3.0 mL of 0.01 M NaCl (A) with  $2.0 \mu\text{g mL}^{-1}$  protamine and  $30 \mu\text{L}$  of functionalized magnetic beads in the presence of 0 (a),  $10^{-10}$  (b),  $10^{-9}$  (c),  $10^{-8}$  (d),  $10^{-7}$  (e), and  $10^{-6}$  M BPA. (C) Potential changes over the BPA concentration range of  $10^{-10}$ – $10^{-6}$  M measured at 80 s after incubated test solutions were injected. (D) Potential differences between the baseline and the potentials measured at 80 s after incubated test solutions were injected for different targets: (a)  $10^{-6}$  M bisphenol A; (b)  $10^{-4}$  M phenol; (c)  $10^{-4}$  M 2-phenylphenol; (d)  $10^{-4}$  M bisphenol A dimethacrylate; (e)  $10^{-4}$  M 4,4'-dihydroxybiphenyl. Error bars represent one standard deviation for three measurements. Unless stated otherwise, the other conditions are as given for protocol C.

to the target molecules (Figure 1C). Using protocol C, the potential responses to BPA at different concentrations are shown in Figure 4B. A linear potentiometric response can be observed over the concentration range of 0.1 to 100 nM (Figure 4C). The detection limit of BPA was calculated as 80 pM ( $3\sigma$ ), which is much lower than the previously achieved values using an immunoassay method.<sup>30,31</sup> As a control test, a bare magnetic bead without linkage of “supersandwich” structure had no response to BPA (data not shown).

In order to test the specificity of the potentiometric aptasensor for the detection of BPA, a comparison of the responses to phenol, 2-phenylphenol, bisphenol A dimethacrylate, and 4,4'-dihydroxybiphenyl was made. As shown in Figure 4D, the electrode does not show any obvious potential changes when exposed to these analogs. The excellent selectivity of the aptasensor originates from the high-affinity binding of the aptamer to its target molecules. Overall, this potentiometric aptasensor was found to be sensitive and specific to BPA and may have promising potential for future applications in clinical and environmental monitoring.

## CONCLUSIONS

In conclusion, the proposed DNA nanostructure-based potentiometric detection platform provides a simple, general, and sensitive aptasensing strategy. Given the successful applications of polyion sensitive membrane ISE in clinical diagnosis and pharmaceutical analysis and the ability of aptamer to recognize various targets, the method demonstrated here is adaptable to facile detection of a wide range of targets. Moreover, the use of magnetic beads coupled with hybrid-

ization chain reactions allows us to detect targets in complex samples with high sensitivity. Considering the enormous capabilities of oligonucleotides in amplification, we anticipate that our system can also be used for other binding-induced DNA assembly systems.

## ASSOCIATED CONTENT

### Supporting Information

Experimental details and additional information as noted in the text. The Supporting Information is available free of charge on the ACS Publications website at DOI: 10.1021/acs.analchem.5b01576.

## AUTHOR INFORMATION

### Corresponding Author

\*Telephone: +86 535 2109156. Fax: +86535 2109000. E-mail: wqin@yic.ac.cn.

### Notes

The authors declare no competing financial interest.

## ACKNOWLEDGMENTS

This work was financially supported by the National Natural Science Foundation of China (21207156, 41176081), the Instrument Developing Project of the Chinese Academy of Sciences (YZ201161), the Science and Technology Project of Yantai (2012132), the CAS Youth Innovation Promotion Association (2013139), and the Taishan Scholar Program of Shandong Province. We also acknowledge Dr. Xuehua Li from School of Environmental Science and Technology, Dalian University of Technology who provided the software for molecular docking.

## REFERENCES

- (1) Bakker, E.; Pretsch, E. *Angew. Chem. Int. Ed.* **2007**, *46*, 5660–5668.
- (2) Bobacka, J.; Ivaska, A.; Lewenstam, A. *Chem. Rev.* **2008**, *108*, 329–351.
- (3) Bakker, E. *TrAC, Trends Anal. Chem.* **2014**, *53*, 98–105.
- (4) Höfler, L.; Bedlechowicz, I.; Vigassy, T.; Gyurcsányi, R. E.; Bakker, E.; Pretsch, E. *Anal. Chem.* **2009**, *81*, 3592–3599.
- (5) Gemene, K. L.; Meyerhoff, M. E. *Anal. Chem.* **2010**, *82*, 1612–1615.
- (6) Shvarev, A.; Bakker, E. *J. Am. Chem. Soc.* **2003**, *125*, 11192–11193.
- (7) Ding, J. W.; Qin, W. *J. Am. Chem. Soc.* **2009**, *131*, 14640–14641.
- (8) Grygolonowicz-Pawlak, E.; Bakker, E. *Anal. Chem.* **2010**, *82*, 4537–4542.
- (9) Jággerszki, G.; Takács, Á.; Bitter, I.; Gyurcsányi, R. E. *Angew. Chem., Int. Ed.* **2011**, *50*, 1656–1659.
- (10) Chumbimuni-Torres, K. Y.; Calvo-Marzal, P.; Wang, J.; Bakker, E. *Anal. Chem.* **2008**, *80*, 6114–6118.
- (11) Qin, W.; Liang, R. N.; Fu, X. L.; Wang, Q. W.; Yin, T. J.; Song, W. J. *Anal. Chem.* **2012**, *84*, 10509–10513.
- (12) Iliuk, A. B.; Hu, L. H.; Andy Tao, W. *Anal. Chem.* **2011**, *83*, 4440–4452.
- (13) Willner, I.; Zayats, M. *Angew. Chem., Int. Ed.* **2007**, *46*, 6408–6418.
- (14) Numnuam, A.; Chumbimuni-Torres, Y.; Xiang, Y.; Bash, R.; Thavarungkul, P.; Kanatharana, P.; Pretsch, E.; Wang, J.; Bakker, E. *Anal. Chem.* **2008**, *80*, 707–712.
- (15) Zelada-Guillen, G. A.; Riu, J.; Duezguen, A.; Rius, F. X. *Angew. Chem., Int. Ed.* **2009**, *48*, 7334–7337.
- (16) Ding, J. W.; Chen, Y.; Wang, X. W.; Qin, W. *Anal. Chem.* **2012**, *84*, 2055–2061.

- (17) Ding, J. W.; Lei, J. H.; Ma, X.; Gong, J.; Qin, W. *Anal. Chem.* **2014**, *86*, 9412–9416.
- (18) Dirks, R. M.; Pierce, N. A. *Proc. Natl. Acad. Sci. U.S.A.* **2004**, *101*, 15275–15278.
- (19) Huang, J.; Wu, Y. R.; Chen, Y.; Zhu, Z.; Yang, X. H.; James Yang, C. Y.; Wang, K. M.; Tan, W. H. *Angew. Chem., Int. Ed.* **2011**, *50*, 401–404.
- (20) Chen, X.; Hong, C. Y.; Lin, Y. H.; Chen, J. H.; Chen, G. N.; Yang, H. H. *Anal. Chem.* **2012**, *84*, 8277–8283.
- (21) Xu, J.; Wu, J.; Zong, C.; Ju, H. X.; Yan, F. *Anal. Chem.* **2013**, *85*, 3374–3379.
- (22) Zheng, J.; Hu, Y. P.; Bai, J. H.; Ma, C.; Li, J. S.; Li, Y. H.; Shi, M. L.; Tan, W. H.; Yang, R. H. *Anal. Chem.* **2014**, *86*, 2205–2212.
- (23) Liu, N. N.; Jiang, Y. N.; Zhou, Y. H.; Xia, F.; Guo, W.; Jiang, L. *Angew. Chem., Int. Ed.* **2013**, *52*, 2007–2011.
- (24) Tram, K.; Kanda, P.; Salena, B. J.; Huan, S. Y.; Li, Y. F. *Angew. Chem., Int. Ed.* **2014**, *53*, 12799–12802.
- (25) Jo, M.; Ahn, J.; Lee, J.; Lee, S.; Hong, S. W.; Yoo, J. W.; Kang, J.; Dua, P.; Lee, D.; Hong, S.; Kim, S. *Oligonucleotides* **2011**, *21*, 85–91.
- (26) Kambhampati, D.; Nielsen, P. E.; Knoll, W. *Biosens. Bioelectron.* **2001**, *16*, 1109–1118.
- (27) Li, F.; Li, X. H.; Shao, J. P.; Chi, P.; Chen, J. W.; Wang, Z. J. *Chem. Res. Toxicol.* **2010**, *23*, 1349–1355.
- (28) Fu, B.; Bakker, E.; Yun, J. H.; Yang, V. C.; Meyerhoff, M. E. *Anal. Chem.* **1994**, *66*, 2250–2259.
- (29) Prieto, M. C.; Maki, A. H.; Balhorn, R. *Biochemistry* **1997**, *36*, 11944–11951.
- (30) Piao, M. H.; Noh, H. B.; Rahman, M. A.; Won, M. S.; Shim, Y. B. *Electroanalysis* **2008**, *20*, 30–37.
- (31) Ragavan, K. V.; Rastogi, N. K.; Thakur, M. S. *TrAC, Trends Anal. Chem.* **2013**, *52*, 248–260.